Araştırma Makalesi - ***Research Article*** *Türk Coğrafya Dergisi 89 (2026) 93-109*

Türk Coğrafya Dergisi
Turkish Geographical Review
www.tcd.org.tr
Basılı ISSN 1302-5856 Elektronik ISSN 1308-9773

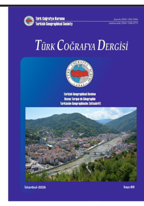

Seismic hazard assessment in active tectonic basins using a AHP-LR model: The case of Tokat (North Anatolian Fault Zone, Türkiye)

Aktif tektonik havzalarda AHP-LR modeli kullanılarak sismik tehlike değerlendirmesi: Tokat örneği (Kuzey Anadolu Fay Zonu, Türkiye)

Ahmet Toprak[a] * Sevilay Yaşarul [b]
[a] Fırat Üniversitesi, İnsan ve Toplum Bilimleri Fakültesi, Coğrafya Bölümü, Elazığ, Türkiye
[b] Fırat Üniversitesi, Sosyal Bilimler Enstitüsü, Coğrafya Bölümü, Elazığ, Türkiye

ORCID: A.T. 0000-0001-6790-1856; S.Y. 0009-0000-7921-0171

BİLGİ / INFO

Geliş/Received: 23.01.2026
Kabul/Accepted: 08.03.2026

Keywords:
Seismic Hazard
Analytic Hierarchy Process
Logistic Regression
Model
Tokat

Anahtar Kelimeler:
Sismik Tehlike
Analitik Hiyerarşi Süreci
Lojistik Regresyon
Model
Tokat

***Sorumlu yazar/Corresponding author:**
(A. Toprak) atoprak@firat.edu.tr

DOI: 10.17211/tcd.1870383

Atıf/Citation: Toprak, A., Yaşarul, S. (2026). Seismic hazard assessment in active tectonic basins using a AHP-LR model: The case of Tokat (North Anatolian Fault Zone, Türkiye). *Turkish Geographical Review*, (89), 93-109.
https://doi.org/10.17211/tcd.1870383

ABSTRACT / ÖZ

The province of Tokat, situated along the North Anatolian Fault Zone (NAFZ), is an active tectonic region that has been subject to destructive earthquakes throughout history. In this study, the seismic hazard potential of Tokat Province has been spatially modelled by integrating the Analytic Hierarchy Process (AHP), based on expert opinion, and data-driven Logistic Regression (LR) methods. The study utilized 11 different parameters, including lithology, fault distance, soil liquefaction, Vs30, slope, and settlement development. To prevent overfitting in the LR model, the number of parameters was statistically reduced to seven key factors. The model was trained using data from areas identified as very high hazard via the AHP. The analysis revealed that the area under the ROC curve (AUC) for the LR model was calculated as 0.952, a value that demonstrates the model's predictive success. Whilst the AHP model classified 30.5% of the province as very low risk, the LR model expanded the hazardous areas, classifying the Erbaa, Niksar and Tokat basins in particular as High Risk. Surface fractures identified during field observations across the province fully correspond with the LR model's high-risk predictions. The resulting model provides a reliable basis for regional disaster management and urban planning strategies.

Kuzey Anadolu Fay Zonu (KAFZ) üzerinde yer alan Tokat ili, tarihsel süreçte yıkıcı depremlere maruz kalmış aktif bir tektonik bölgedir. Bu çalışmada, Tokat ilinin sismik tehlike potansiyeli, uzman görüşüne dayalı Analitik Hiyerarşi Süreci (AHP) ve veri odaklı Lojistik Regresyon (LR) yöntemleri entegre edilerek mekânsal olarak modellenmiştir. Çalışmada litoloji, fay mesafesi, zemin sıvılaşması, Vs30, eğim ve yerleşim gelişimi gibi 11 farklı parametre kullanılmıştır. LR modelinde aşırı uyumu (overfitting) önlemek amacıyla parametre sayısı istatistiksel olarak 7 temel faktöre indirgenmiştir. Modelin eğitimi, AHP ile belirlenen "çok yüksek tehlikeli" alan verileri kullanılarak gerçekleştirilmiştir. Analiz sonucunda, LR modelinin ROC eğrisi altında kalan alan (AUC) değeri 0.952 olarak hesaplanmış olup, bu değer modelin tahmin başarısını göstermektedir. AHP modeli ilin %30,5'ini "çok düşük tehlikeli" olarak tanımlarken, LR modeli tehlikeli alanlarını genişleterek özellikle Erbaa, Niksar ve Tokat havzalarını "Yüksek Tehlikeli" sınıfında değerlendirmiştir. İl geneli gerçekleştirilen saha gözlemlerinde tespit edilen yüzey kırıkları, LR modelinin yüksek tehlikeli tahminleriyle tam örtüşmektedir. Elde edilen model, bölgesel afet yönetimi ve kentsel planlama stratejileri için güvenilir bir altlık sunmaktadır.

Extended Abstract

Introduction

The province of Tokat, which stretches along the North Anatolian Fault (NAF), represents an active tectonic region that has historically been subject to destructive earthquakes. The province is extremely vulnerable not only because it lies on the active sections of the NAF, particularly the Erzincan-Niksar-Erbaa segment, but also due to the seismic wave potential of the alluvial basin deposits. Historical destructive events, particularly the 1942 earthquake (M=7.2) which caused a 50 km surface rupture and necessitated the relocation of the Erbaa district centre, highlight the region's disaster potential. Furthermore, recent rapid urbanization and the concentration of the population in these loose alluvial plains have transformed this natural earthquake risk into an urgent safety issue. In this study, the seismic hazard potential of Tokat Province was assessed using the Analytic Hierarchy Process (AHP), based on expert opinions, and the data-driven Logistic Regression (LR) method. Whilst traditional heuristic models such as AHP are extremely valuable, their integration with data-driven statistical models such as LR significantly enhances the predictive power and spatial accuracy of seismic vulnerability analyses. This approach effectively reduces the subjectivity inherent in expert judgements and eliminates overfitting issues through systematic parameter reduction. In this study, high-risk areas identified using AHP were utilized as a training dataset for the LR algorithm, thereby combining qualitative expert experience with quantitative local datasets.

Data and Method

The analysis utilized eleven different conditioning parameters, including lithology, distance from faults, soil liquefaction, Vs30, slope, and settlement development. To mitigate the issue of overfitting in the LR model, the number of parameters was statistically reduced to seven main factors. The model was then trained using data obtained from areas identified as very high risk via the AHP method. In particular, the initial spatial dataset was sourced from official institutions. The dataset was created using the collected data, and to ensure analytical consistency, all variables were standardised to a spatial resolution of 25×25 m. Whilst the AHP component determines the basic hazard boundaries based on established seismotectonic and geomorphological criteria, the LR model acts as an objective and data-driven filter. Consequently, the use of heuristic model outputs as training samples for statistical models effectively bridges the gap between qualitative expert subjectivity and quantitative spatial prediction, and facilitates the identification of hidden hazard zones that might otherwise be overlooked when relying solely on expert intuition. The AHP method was used to determine the relative weights of the first 11 parameters via pairwise comparison matrices evaluated by experts. The Consistency Ratio (CR) for these matrices was calculated as 3%; this ratio is generally accepted as 10%. remained below the threshold value, thereby ensuring the consistency and reliability of the expert judgements. In the study, a multicollinearity analysis was conducted to construct the LR model, and variables such as Peak Ground Acceleration (PGA), elevation, epicentre distance and number of storeys were systematically excluded to prevent variance inflation and eliminate model redundancy. The remaining seven independent variables distance to faults, epicentre density, soil liquefaction, settlement development, lithology, slope, and Vs30 had Variance Inflation Factor (VIF) values ranging from 1.03 to 2.31. This confirms the absence of multicollinearity. By coding the "Very High" hazard core zones derived from the AHP as '1' (presence of hazard) and other areas as "0" (absence of hazard), this framework has effectively recalibrated the relationships between the factors. Whilst the AHP component determines the basic hazard boundaries based on established seismotectonic and geomorphological criteria, the LR model acts as an objective and data-driven filter. Consequently, the use of heuristic model outputs as training examples for statistical models effectively bridges the gap between qualitative expert subjectivity and quantitative spatial prediction and facilitates the identification of hidden hazard zones that might otherwise be overlooked when relying solely on expert intuition.

Results and Discussion

The analysis revealed an Area Under the Curve (AUC) value of 0.952 for the LR model, indicating excellent predictive performance. In this statistically optimised model, fault distance and epicentre density were identified as the dominant factors determining the hazard distribution. Whilst the AHP model classified 30.5% of the province as Very Low Risk, the LR model expanded the risk zones, specifically including the Erbaa, Niksar and Tokat basins in the high-risk category. In particular, field observations conducted across the province following the 2024 Sulusaray earthquake confirmed that the identified surface fractures fully corresponded with the LR model's high-risk predictions. Spatial distributions revealed distinct differences between expert-based and data-driven approaches. The Analytic Hierarchy Process (AHP) model provided a more cautious framework. The resulting model offers a reliable framework for regional disaster management and urban planning strategies.

1. Introduction

Population growth and unplanned urbanization worldwide have transformed earthquake risk into a global security issue in seismically active regions. The Sendai Framework for Disaster Risk Reduction (2015-2030) prioritizes conducting multi-disciplinary risk analyses at the local scale to build disaster-resilient societies (UNISDR, 2015). Earthquake risk is defined as a function of seismic hazard (ground shaking potential), physical exposure, and structural vulnerability (Varnes, 1984). In this context, determining the seismic characteristics of settlement areas is one of the fundamental components of sustainable urban planning.

More than half of Türkiye's territory is located within the first-degree earthquake zone (Özmen et al., 1997; Özşahin, 2014). Earthquakes are among the most destructive natural disasters, causing significant loss of life and property in affected areas. It is reported that 62% of the damage caused by natural disasters in Türkiye in recent years is due to earthquakes (Marangoz & İzci, 2023). Beyond their initial physical destructiveness, earthquakes have the power to directly affect life in many contexts, ranging from human population and economy to agriculture, tourism, and industry (Özüpekçe & Deniz, 2023). Located on the Alpine-Himalayan seismic belt in the Mediterranean Region, Türkiye is one of the countries with the highest seismic activity in the world. This tectonic setting has led to numerous destructive earthquakes throughout history, causing significant losses, particularly in regions with high population density and uncontrolled urbanization (Özkazanç, 2015; Yavaşoğlu & Özden, 2017; Şeker, 2023). While an average of one earthquake with a magnitude of Mw ≥ 6.0 occurs annually across the country, approximately 25 earthquakes in the 5.0–6.0 range and around 200 in the 4.0–5.0 range are recorded (AFAD, 2024). Recent studies utilizing predictive models chains have further demonstrated that seismic events can accelerate unplanned urban expansion into agricultural lands, significantly altering land use dynamics and increasing long-term vulnerability (Sunbul et al., 2025). The concentration of the population in alluvial plains and unplanned land use are among the primary reasons for the increase in earthquake-related losses in recent years (Sönmez, 2011).

The North Anatolian Fault Zone (NAFZ) is one of the world's most significant and active strike-slip fault zones (Şengör et al., 1985; Şaroğlu et al., 1992; Emre et al., 2013; Alkan et al., 2023). Due to its remarkable kinematic, morphological, and seismogenic similarities, the NAFZ is widely recognized in the international literature as the geological twin of the San Andreas Fault Zone (SAFZ) in California and shares analogous tectonic behaviors with the Alpine Fault in New Zealand (Şengör et al., 2005; Hubert-Ferrari et al., 2002). Therefore, Tokat province, situated directly on the active segments and alluvial basins of the NAFZ, serves as an ideal natural laboratory for assessing seismic hazards. With its right-lateral strike-slip character and the earthquakes it has produced from the past to the present, the NAFZ serves of seismotectonics (Şengör et al., 2005). Tokat province, located on this zone, carries a high hazard potential not only due to the influence of the main fault line but also due to secondary fault branches connected to this main line and the seismic wave amplification potential of basin fills. The districts of Erbaa, Niksar, and Reşadiye, along with the Tokat city center, are situated directly on the NAFZ (Eyidoğan et al., 1991; Susam et al., 2011). The most significant seismic event in these areas was the earthquake dated December 20, 1942. This earthquake, with a magnitude of 7.2, resulted in a surface rupture approximately 50 km long (Tatar et al., 2006). Earthquake-induced damage and loss of life result from the interaction of multiple factors. These include seismological characteristics (e.g., proximity to the epicenter and active faults), geotechnical conditions (e.g., local soil properties), and human-related elements such as site selection, population density, and building quality (Kiper, 2001; Şengün et al., 2018; Toprak & Sunkar, 2022).

In recent years, the Analytic Hierarchy Process (AHP), one of the Multi-Criteria Decision Making (MCDM) methods, and statistical methods have been frequently used in earthquake risk, hazard, and susceptibility analyses (Toprak & Günek, 2016; Hu et al., 2018; Rehman et al., 2024). The most significant advantage of AHP is its simplicity and applicability to various regions (Liberatore & Nydick, 1990). However, literature suggests that Decision Support Systems (DSS) used in seismic susceptibility analyses may sometimes be insufficient in managing uncertainties in expert opinions. At this point, integrating knowledge-based methods like AHP with data-driven statistical models like Logistic Regression (LR) enhances the model's predictive power and spatial accuracy (Pourghasemi et al., 2012; Wang & Li, 2017). This approach offers more reliable decision maps by merging both qualitative expert experience and quantitative local datasets.

The primary aim of this study is to spatially predict the potential earthquake hazard for Tokat province by combining geological, topographic, and anthropogenic parameters and to develop risk mitigation strategies. In this context, a comprehensive, data-driven earthquake hazard map was produced by integrating AHP and LR methods. Eleven variables, including both natural and anthropogenic factors such as Peak Ground Acceleration (PGA), soil liquefaction (Vs30), slope, elevation, distance to faults, distance to the epicenter, lithology, epicenter density, settlement development, and number of building floors, were used to determine earthquake hazard. The inclusion of Vs30 values and PGA data, in particular, transforms the study from a mere geographical analysis into a geotechnical-based seismic micro-zonation background. Eleven parameters were weighted using the AHP method, and the very high hazard areas in the resulting map were used as the dependent variable in the LR model. In the LR analysis, the number of factors was reduced to 7 to eliminate overfitting and multicollinearity issues. The obtained results provide a scientific basis for accurately revealing the spatial distribution of earthquake hazard in Tokat, identifying high-hazard regions, determining urban transformation priorities, and developing disaster management policies.

1.1. Study Area

Tokat Province, located in the Central Black Sea Section of northern Türkiye, is a region characterized by high seismotectonic activity due to its location on the NAFZ (Figure 1).

The NAFZ is not only one of the most significant right-lateral strike-slip fault systems in the world but also the most active tectonic structure in Türkiye (Ambraseys, 1970; Şengör, 1979; Şengör et al., 1985; Barka, 1992). The study area is situated on the Erzincan–Niksar–Erbaa segment of the NAFZ, which has generated numerous destructive earthquakes throughout history. Distinct surface ruptures were observed within the Taşova-Erbaa and Niksar basins resulting from the earthquakes of 1939 (M=7.9), 1942 (M=7.2), and 1943 (M=7.6) (Ardos, 1995; Barka et al., 2000; Akın et al., 2010). Specifically, the 1942 Niksar-Erbaa earthquake caused catastrophic damage in the region, necessitating the relocation of the Erbaa district center further south following the disaster. In addition to tectonic risks, the fact that a significant portion of settlement areas and economic zones are established on loose alluvial deposits is a fundamental factor increasing the earthquake susceptibility of the region.

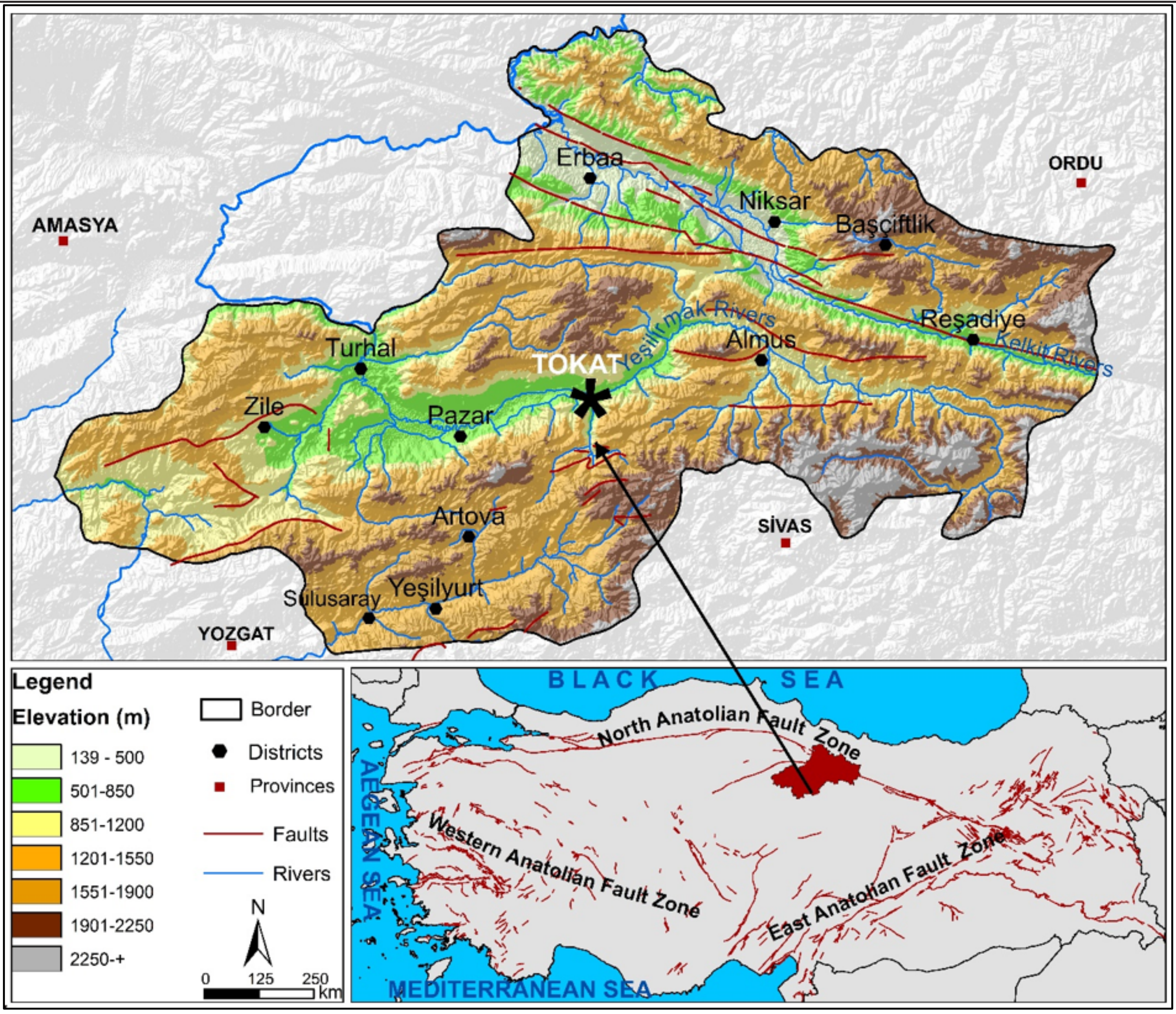

Figure 1. Location and seismicity map of the study area.

2. Methodology

2.1. Data Collection

To identify the parameters influencing seismic hazard in Tokat Province, a comprehensive dataset was constructed utilizing both official institutions and open-source databases. During the data acquisition process, data were obtained from institutional sources such as the Disaster and Emergency Management Presidency (AFAD), Boğaziçi University Kandilli Observatory, the General Directorate of Mineral Research and Exploration (MTA), and the European Commission (JRC), as well as from open-access platforms like Copernicus GLO 30 (FABDEM) (Table 1). All variables used in the model were subjected to a normalization process between 0 and 1 to ensure analytical compatibility and comparability. In the configuration of the LR model, the presence of an earthquake event was coded as “1” and its absence as “0”, adopting a probability-based classification approach. The selection of the 11 main factors included in the analysis (PGA, liquefaction susceptibility, Vs30, slope, elevation, distance to faults, distance to epicenters, lithology, epicenter density, settlement development, and number of building floors) was based on the seismotectonic characteristics of Tokat Province, data availability, and current literature on seismic susceptibility (Pranowo et al., 2024; Li & Shen, 2024). Specifically, for topographic analyses, raster sets with a 25x25 m spatial resolution generated from Copernicus GLO 30 (FABDEM) data were utilized. This multi-source dataset facilitated the integration of the expert-based AHP and the data-driven LR methods, enabling the production of a reliable, region-specific hazard map.

Elevation (m): Elevation is a significant variable in seismic hazard and risk analysis. Topography can influence processes such as local amplification by altering local soil dynamics and seismic wave propagation (Meunier et al., 2007). This factor provides detailed insights into vulnerability (Yunus et al., 2023). Generally, higher elevation areas are less affected by seismic shaking due to greater terrain stability, indicating a negative correlation between elevation and seismic hazard. In this study, FABDEM was used as the digital elevation data. FABDEM is a global elevation map with 30-meter resolution, generated by removing building and tree height artifacts from the Copernicus GLO 30 Digital Elevation Model (DEM) (Hawker et al., 2022). (Figure 2a).

Slope (°): Slope is a critical parameter in seismic hazard mapping and the assessment of settlement safety (Pal et al., 2008; Tudes, 2012; Ocak & Bahadır, 2022). When seismic energy propagates along an inclined surface, it can concentrate, causing higher acceleration and more intense shaking compared to horizontal ground (Işık et al., 2020; Demir & Altaş, 2024). The slope map of the study area was generated through spatial analyses in ArcGIS 10.5 software using the DEM (Figure 2b).

Epicenter Density (events/km²): Epicenter density, which indicates the spatial clustering of past earthquakes, is one of the fundamental indicators used to predict future seismic hazards. The epicenter is the projection on the Earth's surface of the focus point where the energy stored along the fault plane is released (Harff et al., 2016; Canpolat & Bulucu, 2024). The earthquake epicenters and magnitude data used in the analysis were compiled from the online catalogs of the AFAD and Boğaziçi University Kandilli Observatory (AFAD, 2024; KOERI, 2024) (Figure 2c).

Table 1. *Characteristics of Data Triggering Seismic in the Tokat.*

Data Source (Institution / Platform)	Parameter / Factor	Data Type	Resolution / Detail
AFAD & KOERI (Bogazici Univ.)	Seismic Inventory	Point	Compiled from catalogs
Copernicus GLO 30 (FABDEM)	Elevation	Raster	30 m (Resampled to 25 m)
	Slope	Raster	25x25 m
MTA (General Directorate of Mineral Research)	Faults (Emre et al., 2013)	Vector / Raster	Active Fault Map (1:250,000)
	Lithology	Vector / Raster	Digitized from Geological Maps
EOC Geoservice (WSF)	Settlement Development	Vector	WSF Evolution Data
Global Earthquake Model (GEM 2023)	PGA	Raster	2023 Global Seismic Risk Model
Global Liquefaction Susceptibility Map	Liquefaction	Raster	Global Liquefaction Map
JRC (2018) (Triollet et al. 2018)	Number of Building Floors	Raster / Vector	Global Human Settlement Layer

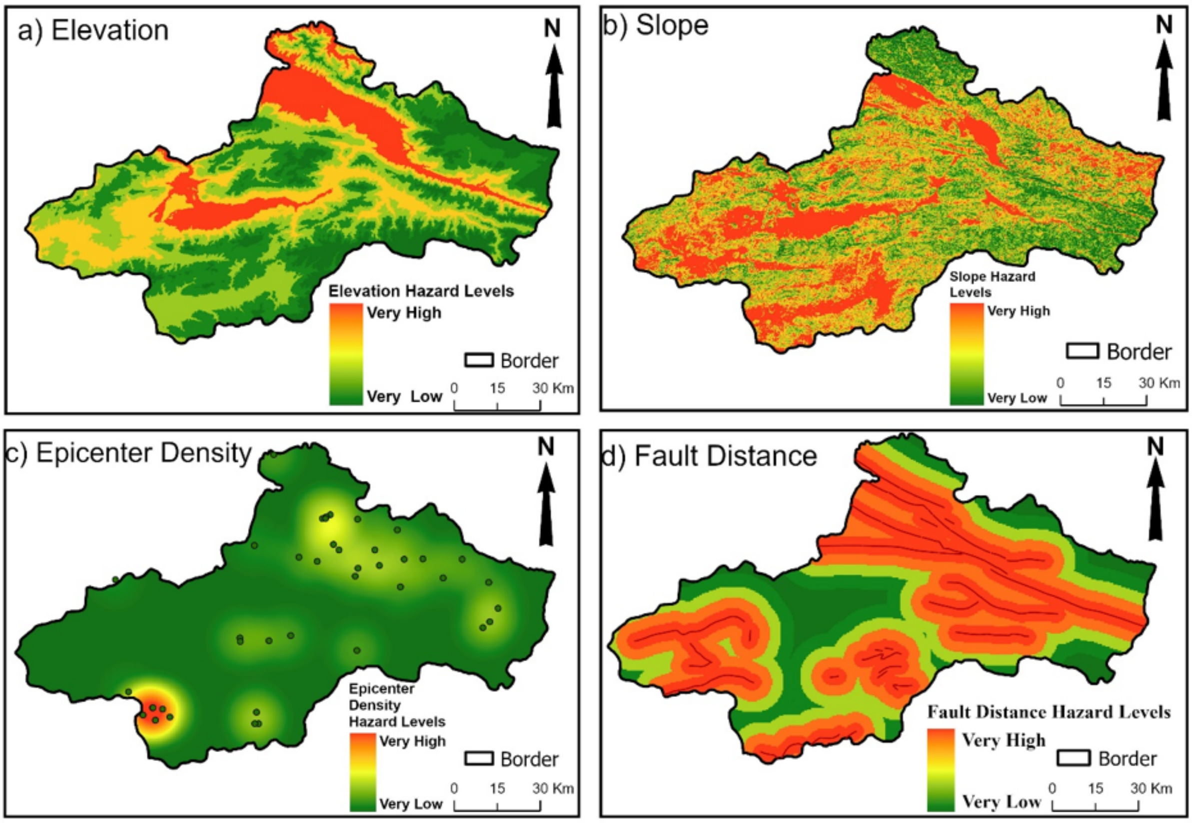

Figure 2. Seismic hazard conditioning factors: a) Elevation, b) Slope, c) Epicenter density, d) Distance to fault lines.

Distance to Faults (km): One of the most critical factors determining damage potential in earthquakes is the distance to fault lines. Proximity to active faults, which are the source of earthquakes, significantly increases the risk of damage, particularly where soil conditions are weak and building resistance is low (Ocak & Bahadır, 2022). Therefore, constructing buildings away from fault avoidance zones is a fundamental strategy in seismic hazard reduction. The fault data used in this study were obtained from the MTA Active Fault Map, processed in a Geographic Information Systems (GIS) environment, and classified using the Euclidean distance method (Emre et al., 2013). (Figure 2d).

Peak Ground Acceleration (PGA) (g): PGA is the largest acceleration amplitude measured on the ground during an earthquake and indicates the severity of the shaking. High PGA values increase the seismic load, particularly in short-period and rigid structural systems, causing high levels of stress and damage in low-rise reinforced concrete buildings (Kalman Šipoš, et al., 2025; Çatkın & Toprak, 2025). PGA can show significant variability even over short distances depending on local soil conditions, leading to different damage levels within the same area (USGS, 2023; Demir & Altaş, 2024). The PGA data used in this study were obtained from the Global Earthquake Model (2023) database (Figure 3e).

Distance to Epicenter (km): This parameter represents the distance of any point within the study area to historical earthquake epicenters. The epicenter is the projection on the Earth's surface of the focus point where the earthquake originated deep underground (Ochoa et al., 2018; Canpolat & Bulucu, 2024). The proximity of a settlement to the earthquake epicenter is a fundamental factor determining the level of seismic energy exposure and destructive impact. The dataset was derived from the AFAD Earthquake Catalog and generated using distance analysis tools in a GIS environment (Figure 3g).

Settlement Development (Year): A significant portion of settlements in Türkiye has historically developed in high-disaster-probability plains due to factors such as agricultural productivity and ease of transportation. The spatial expansion and construction history of settlements play a critical role in their interaction with seismic events. Heterogeneity in building stock and infrastructure deficiencies, especially in regions undergoing rapid urbanization, are factors that exacerbate earthquake damage. The age of the settlement is directly correlated with infrastructure degradation; indeed, the fatigued building stock and aging infrastructure in older neighborhoods are more vulnerable to seismic events (Ren et al., 2024). In this study, settlement development data were obtained from the EOC Geoservice World Settlement Footprint Evolution dataset (Figure 3f).

Ground Liquefaction: Liquefaction is one of the most critical factors causing soil-related damage during earthquakes. It occurs when water-saturated cohesionless soils lose their shear strength during seismic shaking and behave like a viscous liquid (Alpaslan, 2013). Due to repeated cyclic loading during an earthquake, pore water pressure increases, and effective stress decreases, weakening the bonds between soil particles. As the soil loses its bearing capacity and exhibits fluid-like behavior, it can cause severe damage such as settlement, tilting, or collapse of building foundations (Robertson & Wride, 1998; Orhan & Ateş, 2011). Particularly in urban areas, liquefaction in soft and saturated soils poses a direct threat to structural stability (Mhaske & Choudhury, 2010). The soil liquefaction data used in this study were obtained from the global liquefaction susceptibility map. (Figure 3h).

Number of Building Floors: The number of building floors is a primary parameter determining the dynamic response of structures under seismic loads and their structural resistance performance (Bahadori et al., 2017; Alizadeh et al., 2018; Nazmfar, 2019; Shafapourtehrany et al., 2022). According to TUIK (Turkish Statistical Institute) data, while 83,364 of the 191,711 buildings in the province were constructed in 2001 or later, more than half of the building stock pre-dates the year 2000. Existing buildings typically consist of a ground floor plus 5 or 6 stories (Photo 1). The city center is situated on the "Kazova" basin, a tectonic depression formed during the Eocene epoch (Cankar, 2014). The majority of the population and urbanization is concentrated on this basin floor, which has the potential for seismic wave amplification. While 4–7 story reinforced concrete structures dominate the valley floor, 1–3 story low-density settlements are prevalent on the slopes and foothills. This distribution indicates that geological and geomorphological characteristics directly shape the urban form and, consequently, the distribution of seismic hazard.

Structures exhibit different seismic responses depending on their number of stories. Although literature suggests that seismic vulnerability may increase with the number of stories (Arnold, 2006), there is not always a direct linear correlation between building height and damage risk. The decisive factor is the quality of structural design. High-rise buildings that are not designed according to engineering principles or are constructed with poor quality materials have a significantly higher potential for damage in probable earthquakes (Panahi et al., 2014; Yavaşoğlu & Özden, 2017). The building story data used in this study were obtained from the European Commission Joint Research Centre (JRC, 2018; Triollet et al. 2018) data catalogue (Figure 4ı).

Vs30 (m/s): Vs30 is the average shear wave velocity of soil layers down to a depth of 30 meters. While high Vs30 values represent hard rock environments where seismic waves are attenuated, low values indicate soft soils where site amplification and resonance effects become more pronounced (Rusydi & Efendi, 2018). Vs30 is a fundamental parameter used in the assessment of dynamic soil behavior in international and national standards such as the Uniform Building Code (UBC), Eurocode 8 (EC8), and the Turkish Building Earthquake Code (TBEC) (Akgül & Akın, 2023). The Vs30 data used in this study were obtained by mosaicking the USGS Global Vs30 dataset (Figure 4j).

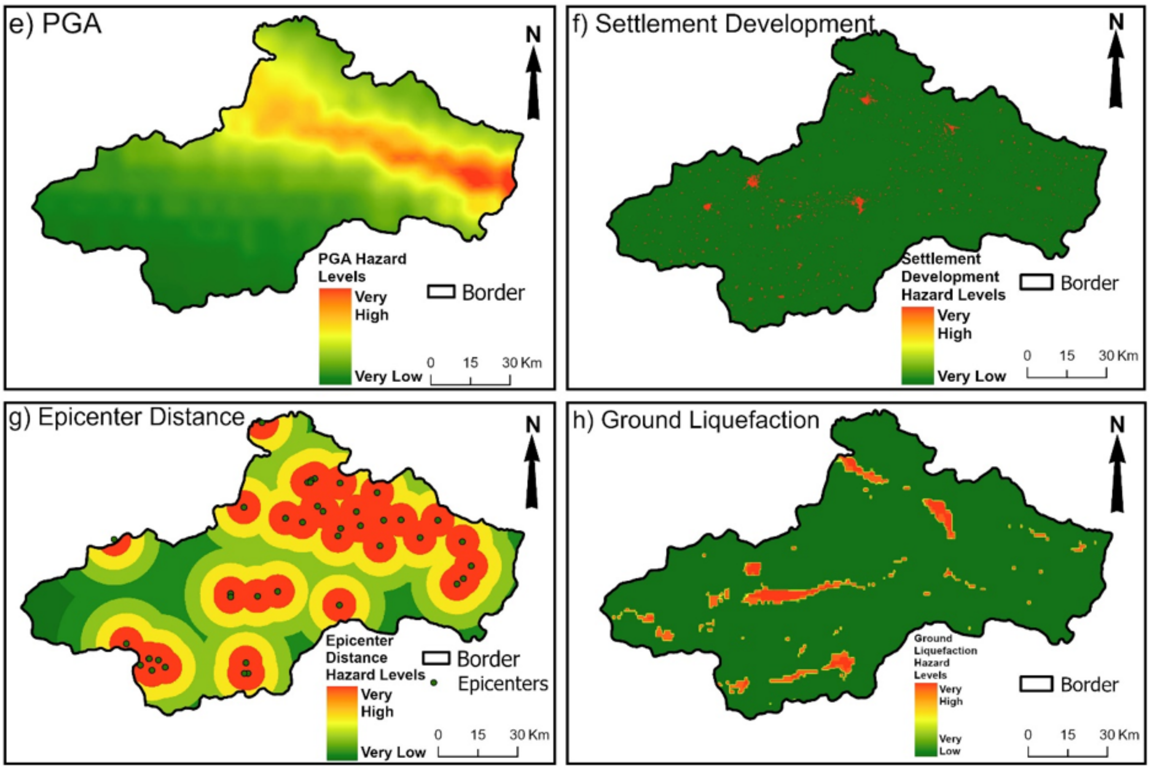

Figure 3. Seismic hazard conditioning factors: e) PGA, f) Settlement development, g) Distance to epicenter, h) Soil liquefaction.

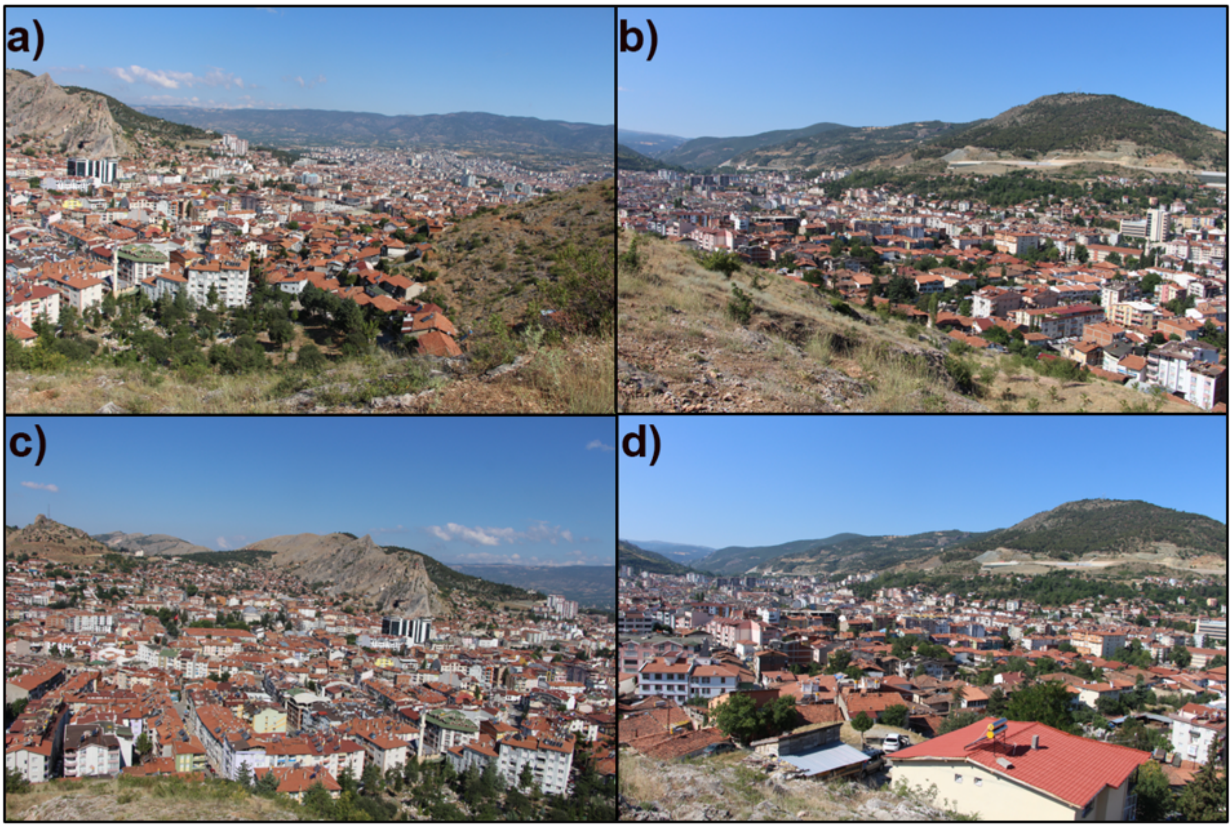

Photo 1. The relationship between building stock and topography and its spatial distribution in Tokat city center.

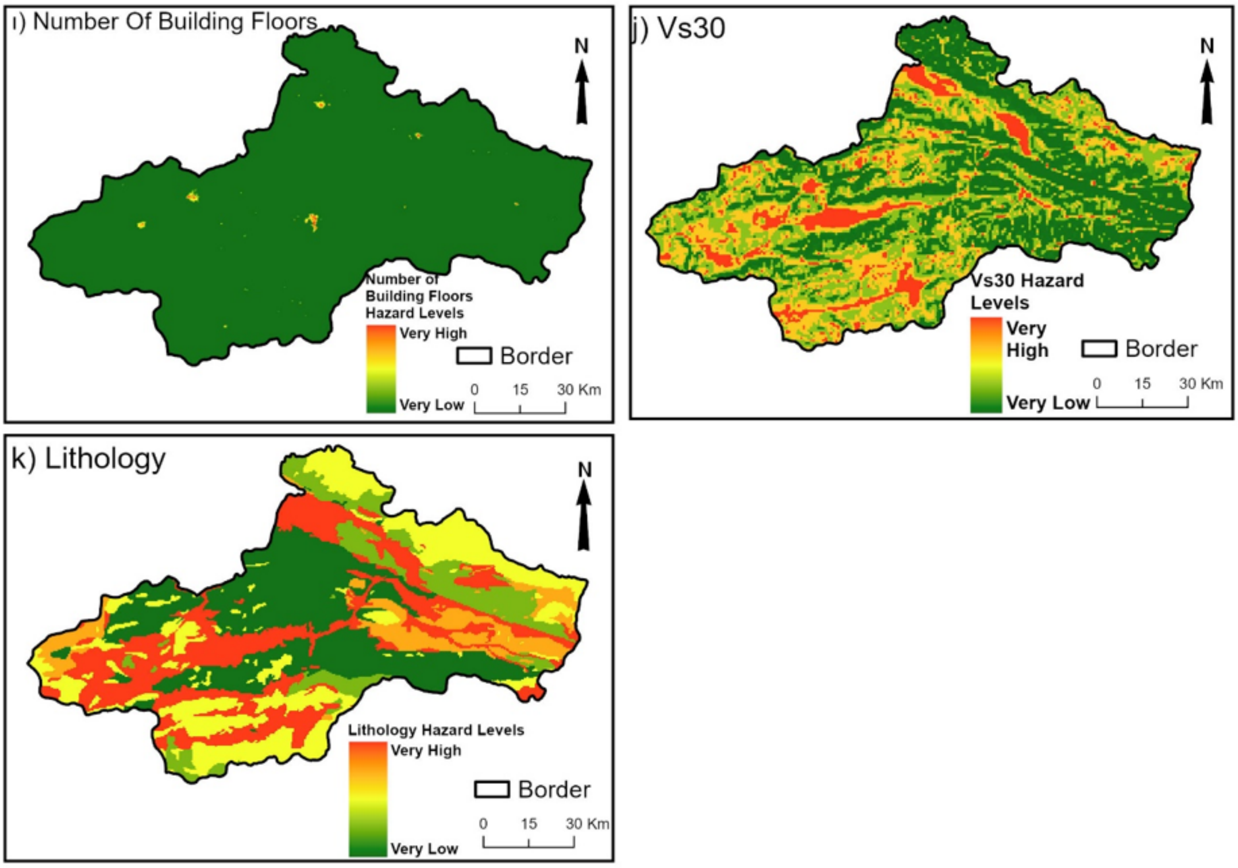

Figure 4. Seismic hazard conditioning factors: ı) Number of building floors, j) Vs30, k) Lithology.

Lithology: Lithology plays a decisive role in the intensity of the earthquake on the surface and the level of damage by either amplifying or attenuating seismic waves (Erinç, 2000). As a general rule, damage risk is observed to be lower in structures built on hard and consolidated rock types such as basalt and andesite. Conversely, it is known that higher damage potential occurs in loose or weakly cemented sedimentary units such as clay, silt, and sandstone (Siyahi et al., 2013). The lithology data used in this study were generated by digitizing MTA geological maps and reclassified according to soil strength properties. The Tokat city center, which has developed on a fault-controlled valley floor, is surrounded by sloping hillsides composed of limestone and volcanic units (Photo 2; Figure 4k).

Photo 2. Tokat city center: Settlement pattern located on a fault-controlled valley floor.

2.2 Analytic Hierarchy Process (AHP)

The AHP, proposed by Saaty (1980), is one of the most popular Multi-Criteria Decision Making (MCDM) methods. It provides a systematic and consistent analytical framework that allows for determining the relative importance of decision elements within a hierarchical structure (Saaty, 1980). AHP offers an easily applicable and understandable structure as it can be applied to numerous criteria without requiring complex mathematical calculations. Its ability to calculate the consistency of pairwise comparisons and represent the decision problem hierarchically makes it a suitable method for group decision-making (Özbek, 2017). To minimize errors in the study, each parameter was resampled to a common resolution using appropriate interpolation methods.

2.3 Logistic Regression Analysis (LR)

LR is one of the most popular supervised statistical methods. LR is frequently preferred over other methods for explaining relationships between variables, particularly when the dependent variable is categorical, as it imposes no restrictions on whether independent variables are continuous or discrete (Bulut, 2023). As a multivariate statistical analysis model, it is used to predict the presence or absence of a specific characteristic based on the values of a set of control factors (Xie et al., 2018). The primary objective of LR analysis is to construct a model with the best fit using the fewest variables to define the relationship between the dependent variable and the set of independent variables (Aktaş & Erkuş, 2009). Its most significant advantage is that the data do not require a normal distribution.

In this study, a comprehensive methodological workflow based on the integration of AHP and LR models was established (Figure 5). Maps of 11 main factors reflecting the province's seismotectonic and morphological characteristics were converted to the same pixel size (25x25 m) as the Digital Elevation Model. All these maps were standardized using ArcGIS Pro 3.5.0 software and weighted via AHP pairwise comparison matrices constructed based on expert opinions. In the second stage, a modeling strategy was adopted to enhance prediction accuracy and address multicollinearity issues. For this purpose, very high hazard areas identified by the AHP model were used as the dependent variable in the LR analysis. In the LR analysis, the dependent variable was coded as 1 (presence of high hazard defined by AHP) and 0 (absence) (Xie et al., 2018).

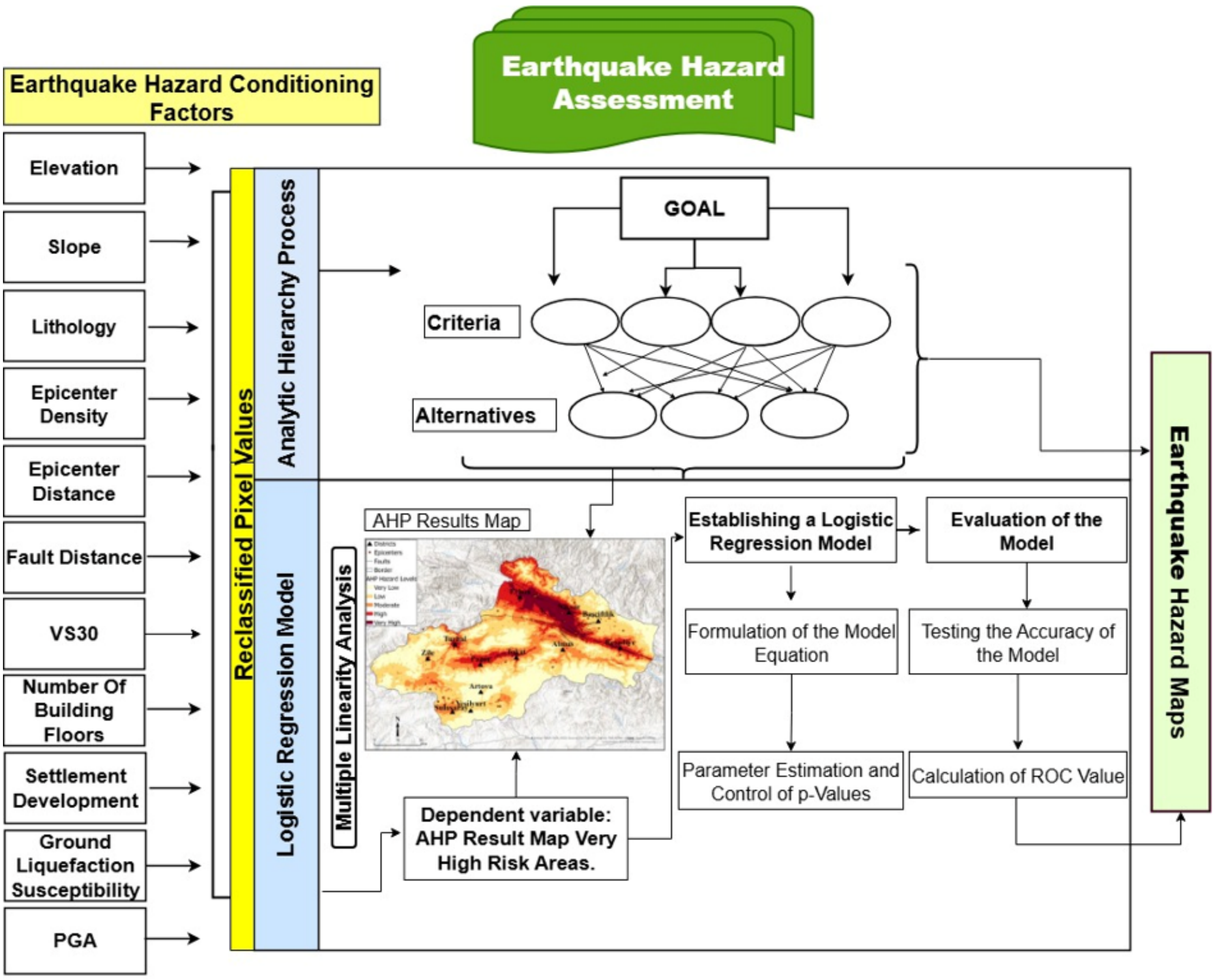

Figure 5. Flowchart of the methodology.

In conventional spatial hazard modeling, historical earthquake epicenters are typically utilized as the primary dependent variables. However, since epicenters represent discrete point data, they inherently fail to capture geotechnical realities that exhibit spatial continuity at the basin scale, such as seismic wave amplification and liquefaction susceptibility. To circumvent this spatial constraint and the problem of under representative sampling, the 'Very High' hazard core zones derived from the expert-based AHP were employed as the training inventory for the LR algorithm. Integrating these AHP-derived regions with LR has been demonstrated to yield superior predictive performance compared to standalone models (He et al., 2023). This methodological framework does not constitute circular reasoning; rather, it ensures the comprehensive projection of all governing parameters onto the final hazard map. While the AHP component delineates the fundamental hazard boundaries based on established seismotectonic, geomorphological, and physical geographic criteria, the LR model functions as an objective, data-driven filter. This algorithm mathematically recalibrates the inter-factor relationships and projects these optimized latent geotechnical patterns across the entire basin. As substantiated in contemporary literature (Pourghasemi et al., 2012; Wang & Li, 2017; He et al., 2023), utilizing heuristic model outputs as training samples for statistical models effectively bridges the gap between qualitative expert subjectivity and quantitative spatial prediction. Consequently, this approach facilitates the identification of 'latent' hazard zones that might be overlooked when relying solely on expert intuition.

3. Results and Discussion

3.1. AHP Analysis and Parameter Weights

The pairwise comparison matrices were constructed based on the opinions of nine experts, primarily from the disciplines of physical geography, seismology, and geology, taking into account existing literature. The calculated Consistency Ratio (CR) was found to be 3% (0.03). Being below the generally accepted threshold of 10% (0.10), this ratio indicates that the expert judgments are consistent and the derived weights can be reliably used in the analysis (Figure 6). According to the calculated weight values, PGA was identified as the most dominant parameter determining seismic hazard, with a weight score of 0.217. This was followed by Liquefaction (0.190) and Distance to Faults (0.165), respectively, while Slope and Vs30 parameters received relatively lower weight values in the expert evaluation.

It is observed that the weight coefficients obtained from the AHP model largely coincide with the seismotectonic and geomorphological realities of the region. The fact that the Consistency Ratio (CR) remained within the 1% to 5% range (CR < 0.10) in all evaluation matrices demonstrates the high consistency of expert judgments and the precision of the scoring process. In particular, the high weight values assigned to the most critical sub-classes of the PGA (0.377) and Vs30 (0.337) parameters indicate a critical level of seismic wave amplification and liquefaction hazard in alluvial-filled grounds throughout the province, specifically in the Niksar, Erbaa, and Tokat central plains (Table 2).

Upon examining the earthquake hazard map produced via the AHP method, it is observed that the districts of Erbaa, Niksar, and Reşadiye fall into the very high hazard category due to their liquefaction potential, earthquake density, and proximity to active faults. This spatial distribution parallels the historical destructive earthquakes in the region (Figure 7). Conversely, the districts of Artova and Yeşilyurt were identified as the areas with the lowest seismic hazard.

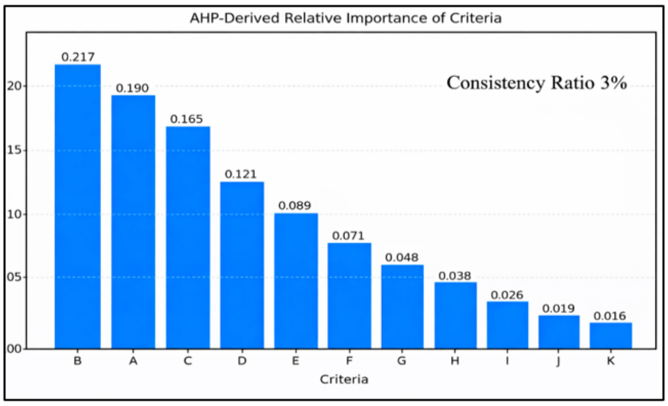

Figure 6. AHP pairwise comparison weights: A) Liquefaction, B) PGA, C) Distance to faults, D) Lithology, E) Epicenter density, F) Settlement development, G) Number of building floors, H) Distance to epicenter, I) Elevation, J) Slope, K) Vs30.

***Table 2**. Sub-criteria Weight Coefficients of the Factors Used in Seismic Hazard Analysis According to the AHP.*

Factor/ Consistency	No. of classes	Interval range (min–max)	Min weight	Max weight	Dominant hazard level
Elevation (CR%1)	5	0 – >800 m	0.176	0.231	Very High
Slope (CR%2)	5	0 – 12.1°	0.091	0.307	Very High
PGA (CR%3)	5	0.1 – 0.7 g	0.109	0.377	Very High
Vs30 (CR%5)	5	180 – 900 m/s	0.135	0.337	Very High
Epicenter density (CR%3)	5	0.001 – 0.029	0.123	0.396	Very High
Distance to epicenter(CR%1)	5	0 – 41.1 km	0.148	0.231	Very High
Distance to faults (CR%4)	5	0 – 80.3 km	0.105	0.252	Very High
Settlement development (CR%4)	5	0 – 2015	0.058	0.317	Very High
Number of building floors (CR%5)	5	0 – 19.8	0.063	0.331	Very High
Lithology (CR%5)	5	Class 1 – Class 5	0.063	0.386	Very High
Liquefaction (CR%4)	5	0.5 – 5.0	0.085	0.297	Very High

The minimum and maximum subclass weights were derived from Analytic Hierarchy Process (AHP) pairwise comparison matrices. Consistency ratios (CR) for all factors were below the acceptable threshold of 0.10.

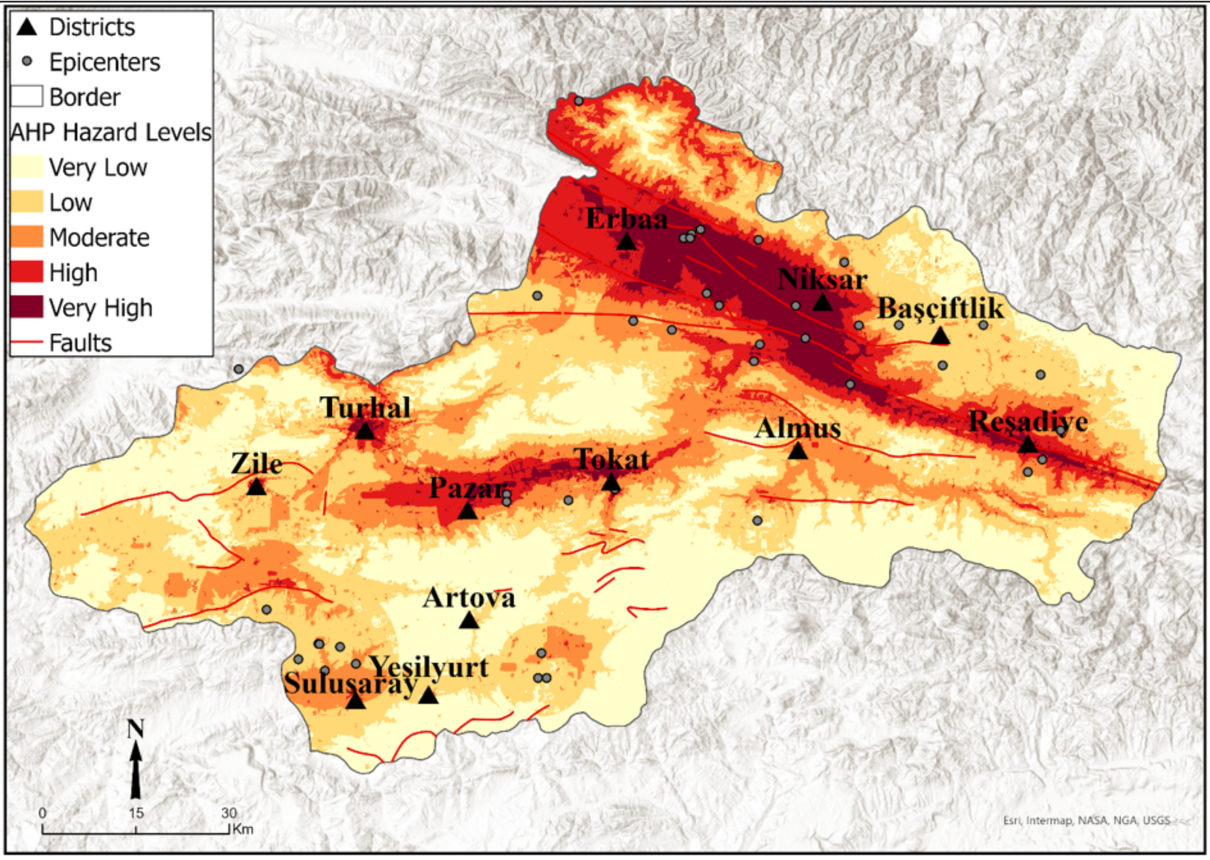

Figure 7. AHP-based earthquake hazard map of Tokat province.

3.2. Logistic Regression Analysis and Results

Within the scope of the LR analysis, the relationship between independent variables and the dependent variable (high-hazard areas) was modeled. According to the classification table (confusion matrix) indicating the model's prediction performance, in cases where hazard was absent (0), 8,803 points were correctly classified, and 1,197 were misclassified, resulting in an accuracy rate of 88.0%. In cases where hazard was present (1), 8,988 points were correctly predicted, while 1,012 were misclassified, achieving a success rate of 89.9%. Consequently, the model's success in identifying earthquake-prone areas (sensitivity) is 89.9%, its success in identifying non-prone areas (specificity) is 88.0%, and the overall accuracy of the model is 89.0% (Table 3).

According to the LR model results, Distance to Faults was identified as the most influential factor, having the highest positive coefficient (B = 11.54). This is followed by Epicenter Density as the second most critical factor with a coefficient of 9.48. Liquefaction (B = 5.38) and Settlement Development (B = 4.86) also exhibited high coefficients, indicating a significant impact within the model. The coefficients for Lithology (B = 2.42), Slope (B = 1.92), and Vs30 (B = 1.60) were also found to be positive. When the Wald statistics, which measure the significance of each variable's contribution to the model, were examined, Distance to Faults (2917.39) and Epicenter Density (2775.57) yielded the highest values. The Exp(B) values presented in the table indicate the fold increase in hazard probability associated with a one-unit increase in the respective variable (Table 4).

***Table 3.** Classification Table of Variables.*

Observed	Predicted		
	Earthquake		Percentage Correct
	0	1	
No Earthquake 0	8803	1197	88.0
Earthquake 1	1012	8988	89.9
Overall Accuracy (%)			89.0

***Table 4.** Estimated Coefficients of Factors Triggering Earthquakes in Tokat Province According to the LR Model.*

Variables in the Equation							
		B	S.E.	Wald	df	Sig.	Exp(B)
Step 1[a]	Vs30	1.607	.135	142.361	1	.000	4.989
	Settlement Development	4.864	.191	645.460	1	.000	129.482
	Liquefaction	5.382	.211	648.400	1	.000	217.479
	Slope	1.924	.251	58.593	1	.000	6.850
	Distance to faults	11.549	.214	2917.396	1	.000	103641.604
	Epicenter density	9.483	.180	2775.575	1	.000	13134.991
	Lithology	2.422	.075	1053.765	1	.000	11.264
	Constant	-16.839	.328	2643.125	1	.000	.000

To enhance the interpretability of the logistic regression model and avoid black-box behavior, the standardized coefficients were visualized using a coefficient bar chart (Figure 8). The results clearly demonstrate that distance to faults is the most influential parameter controlling seismic hazard probability, followed by epicenter density. These two variables reflect the dominant tectonic control of the North Anatolian Fault Zone.

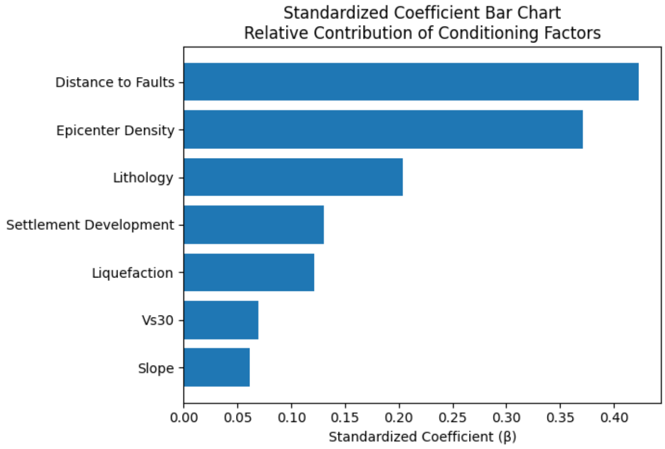

Figure 8. Standardized coefficient bar chart illustrating the relative contribution of conditioning factors in the logistic regression model.

Lithology and settlement development exhibit moderate contributions, highlighting the combined role of geological and anthropogenic factors. In contrast, Vs30 and slope present lower standardized coefficients; however, their positive influence confirms their role as secondary amplifiers of ground motion, particularly within alluvial basins. This visualization provides a transparent and physically interpretable understanding of the model structure.

Upon examining the standardized coefficients (Beta) of the model, Distance to Faults (0.423) and Epicenter Density (0.371) stand out as the factors with the highest impact levels. The positive coefficient of the Vs30 variable confirms the amplifying effect of soil structure on seismic hazard. The VIF (Variance Inflation Factor) values, calculated to test for multicollinearity among variables, range between 1.03 and 2.31. In statistical literature, it is required that VIF values be less than 5 (or 10, according to some sources) and Tolerance values be above 0.10. The analysis results indicate that all variables meet these threshold values and that there is no multicollinearity problem in the model (Table 5). Furthermore, the observation of the highest Condition Index value in the dimension associated with fault distance aligns with the fact that seismic hazard in Tokat province is primarily controlled by active fault zones.

Out of the initial eleven-parameter ensemble, the variables comprising PGA, Elevation, Distance to Epicenter, and Floor Count were systematically pruned from the LR model following a rigorous multicollinearity analysis. The exclusion of PGA is particularly striking given its hierarchical dominance within the AHP framework; yet, its formidable correlation with distance to fault rendered it statistically redundant. In the context of LR modeling, incorporating dual inputs that mirror the same underlying physical signature precipitates overfitting akin to over-stimulating a neural pathway with redundant signals. By distilling these variables, we successfully mitigated VIF thresholds, effectively preventing the model from 'memorizing' the idiosyncrasies of the training set. This strategic reduction fostered a parsimonious yet powerful architecture, significantly enhancing the model's generalization capacity for predictive mapping across broader spatial domains.

It is observed that very-high and high-hazard areas are distinctly concentrated along the NAFZ traversing the northern part of Tokat. While hazard levels in the vicinity of Almus and Turhal are predominantly high and moderate, low and very low hazard classes prevail in the zile and artova districts. Conversely, the districts of Erbaa, Niksar, and Reşadiye, located directly on the NAFZ, fall within the very high-hazard category (Figure 9).

During the training phase of the LR algorithm, areas identified as very high hazard by the AHP method were introduced as the dependent variable, allowing the model to predict other potential hazard areas with similar geo-environmental characteristics. The fact that the LR model successfully identifies these high-hazard zones and consistently models the hazard distribution demonstrates the spatial accuracy of the method.

Field observations conducted in Buğdaylı Village, the epicenter of the Mw 5.6 earthquake that occurred in Tokat-Sulusaray in 2024, provided physical evidence supporting the generated hazard maps. The surface ruptures and tension cracks observed in the study area clearly demonstrate the active tectonic deformation. The fact that the LR model classified this specific area as high hazard demonstrates the model's capability to successfully predict potential earthquake damage zones by capturing active tectonic processes, rather than relying solely on historical data (Photo 3).

***Table 5**. LR Model Coefficients and Multicollinearity Statistics of Seismic Hazard Conditioning Factors in Tokat Province.*

Coefficients[a]								
Model		Unstandardized		Standardized	t	Sig.	Collinearity Statistics	
		B	Std. Error	Beta			Tolerance	VIF
1	(Constant)	-.923	.021		-43.701	.000		
	Vs30	.132	.013	.069	10.015	.000	.433	2.312
	Settlement	.321	.011	.130	28.099	.000	.968	1.033
	Liquefaction	.313	.015	.121	20.506	.000	.593	1.686
	Slope	.256	.026	.061	9.953	.000	.556	1.800
	Distance to faults	.862	.010	.423	83.627	.000	.804	1.244
	Epicenter density	1.008	.014	.371	74.247	.000	.826	1.211
	Lithology	.253	.006	.204	40.609	.000	.818	1.222
a. Dependent Variable: CID								

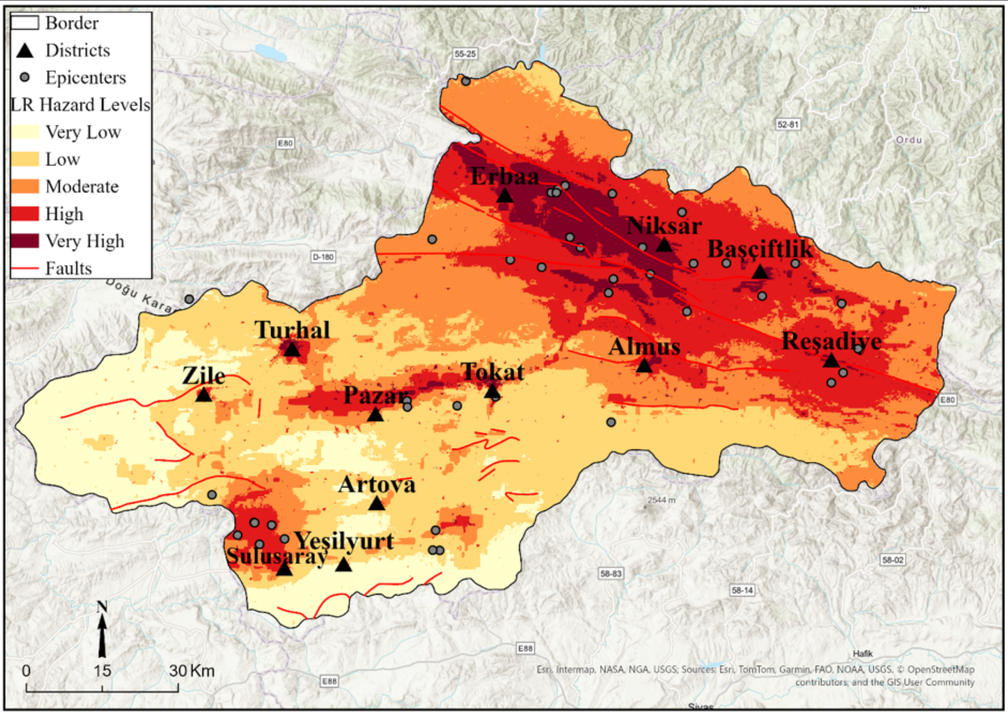

Figure 9. LR based earthquake hazard map of Tokat province.

Photo 3. Surface ruptures and ground deformations observed in Tokat province, Sulusaray-Buğdaylı Village.

The total area of the province is 10,042 km². According to the AHP results, a significant portion of the province (6,577 km²) falls into the low and very low hazard classes. This indicates that the expert judgments in the AHP model tend to exhibit a more conservative approach, classifying the region generally as safer. In contrast, in the LR model, the hazard distribution shifted towards moderate and high classes, characterizing the region as more hazardous compared to AHP.

In the very high hazard zones of the study area, both methods yielded very similar results (Figure 10). This demonstrates that the most prominent hazard sources in the field (proximity to fault lines and weak soils) were successfully detected by both methods. However, in high hazard areas, the LR method identified more than twice the area as hazard compared to AHP. Since the LR algorithm was trained with the very high hazard core data identified by AHP, it may have revealed that certain soil or topographic features, evaluated as moderate hazard in expert opinion, actually carry a high hazard statistically.

Reducing the 11 criteria used in the AHP model to 7 key factors in the LR model to prevent overfitting has revealed the fundamental hazard structure of the region more clearly. The large number of parameters used in the AHP model resulted in a more spatially constrained hazard pattern. In contrast, the LR model, based on seven fundamental variables, identified broader potential hazard zones.

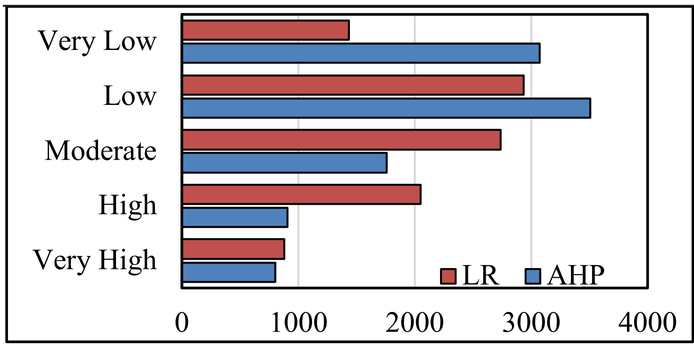

Figure 10. Areal distribution of seismic hazard classes according to AHP and LR models.

As a result of the ROC (Receiver Operating Characteristic) curve analysis conducted to evaluate the predictive performance and spatial accuracy of the LR model, the Area Under the Curve (AUC) value was calculated as 0.952 (Figure 11). In statistical literature, AUC values between 0.9 and 1.0 are considered to represent excellent classification success (Kanık & Erden, 2003). This high accuracy rate proves that there is a strong spatial correlation between the dependent variable used in model training and the independent variables. The fact that the model achieved such high success despite the reduction of parameters from 11 to 7 demonstrates that the generated seismic hazard map constitutes a reliable, consistent, and high-precision basis for spatial planning and disaster hazard reduction strategies.

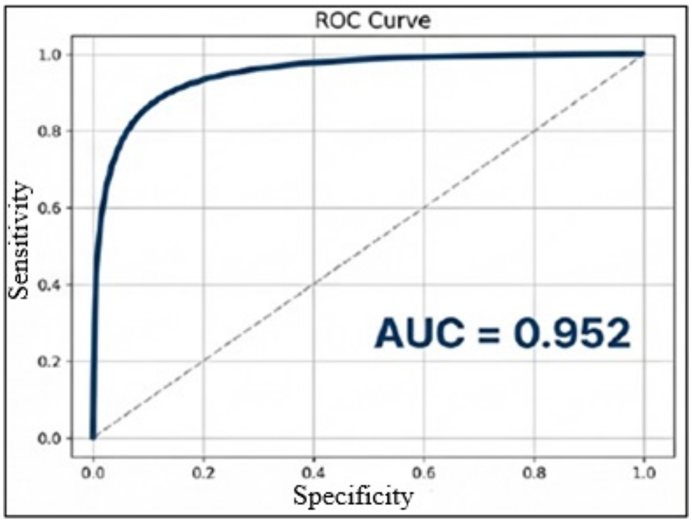

Figure 11. ROC curve representing the performance evaluation of the LR model.

ML models yield high predictive accuracy, they inherently operate as black boxes, often failing to provide a physical explanation for the relative influence of seismic parameters. Conversely, the AHP-LR model developed in this research offers a transparent interpretability by providing standardized coefficients for each factor, as depicted in Figure 8. This methodological transparency establishes an actionable framework for disaster management authorities and urban planners, enabling evidence-based decision-making through a quantifiable understanding of risk drivers.

In this study, a seismic hazard assessment was conducted using integrated AHP and LR methods for Tokat province, which is located on the NAFZ and has been exposed to destructive earthquakes throughout history. The most striking aspect of the study is the difference in spatial distribution between the AHP and LR models. While the expert-based AHP model classified a significant portion of the study area as low hazard, the data-driven LR model expanded the moderate and high hazard classes to a wider area. This situation parallels modeling studies in the literature; indeed, Pourghasemi et al. (2012) and Alizadeh et al. (2018) stated that statistical methods (LR) produce more generalizable results by minimizing uncertainties compared to expert-based methods (AHP).

While AHP is constrained by the top-down subjectivity of expert judgment, the LR model functions as an integrative decoder of latent geotechnical signals specifically basin amplification and liquefaction susceptibility. Validated against the 2024 Sulusaray field data, the LR algorithm successfully filtered heuristic bias to map critical hazard zones in the Erbaa and Niksar basins, extending hazard boundaries beyond immediate fault lines to incorporate vital site-effect dynamics.

In the study, the number of factors was reduced from 11 to 7 in the LR model to prevent overfitting and resolve the multicollinearity problem. While the 11 factors in the AHP model spatially confined the hazard to more specific areas, the 7 fundamental factors (Vs30, distance to faults, lithology, etc.) used in the LR model revealed the fundamental hazard structure of the region. This approach aligns with the principle of capturing the best fit with the fewest variables stated by Xie et al. (2018). The training of the LR model with the very high hazard areas identified by AHP (802 km²) demonstrates that the statistical model successfully learned the core hazard areas (with 89% accuracy) while also expanding the hazard boundaries with a geological buffer zone logic. In this context, LR results provide a safer basis for worst-case scenario planning in disaster management.

The regions identified as very high hazard zones specifically the alluvial basins within Erbaa and Niksar must be designated as priority sectors for localized 1/1000-scale micro-zonation and geological-geotechnical investigations essential for urban land-use planning. The AHP-LR model serves as a strategic decision-support tool, optimizing the spatial allocation of costly borehole operations across extensive study areas. For the high-hazard settlements situated on the 'Kazova' plain in the Tokat provincial center, Urban Transformation Strategic Documents must be updated by cross-referencing building inventory data (structural age, story count) with the outputs of this hazard map. In particular, policies regarding the structural retrofitting of the existing 4-to-7-story building stock in areas with high liquefaction potential should be substantiated by this model's predictive data. Furthermore, the high-accuracy map (AUC: 0.952) presented in this study establishes a rigorous scientific foundation for disaster response logistics and the strategic relocation of post-earthquake assembly points to low-hazard territories, such as the vicinities of Artova and Yeşilyurt.

4. Conclusion

The analysis indicates that high- hazard areas are concentrated in the Erbaa, Niksar, and Tokat central plains. These areas are located on Quaternary alluvial fills and are characterized by low Vs30 values (180-394 m/s) and high liquefaction potential. Our findings coincide with the fact emphasized Ansal et al. (2010) that soft soils increase structural damage by amplifying seismic waves. In particular, the fact that distance to faults and epicenter density parameters have the highest coefficients in the LR model confirms that seismic hazard follows a linear corridor along tectonic lines (Şengör et al., 2005; Tatar et al., 2006). The overlap of alluvial soils covering valley floors with settlement areas proves that the hazard has not only a geological but also a geomorphological origin (Sönmez, 2011).

It is observed that settlements in Tokat province are concentrated on high and very high hazard areas. It is a critical planning issue that the districts of Erbaa and Niksar, in particular, continue to develop on plain floors carrying active fault zones and liquefaction hazard, despite having experienced great destruction in the 1939, 1942, and 1943 earthquakes (Barka, 1996; Üzen, 2014). The inclusion of settlement development and number of building floors factors in our analysis has combined the physical dimension of seismic hazard with the human dimension. As stated by Yoloğlu & Zorlu (2024) and Çatkın & Toprak (2025), rapid urbanization processes in Türkiye generally develop on fertile agricultural lands and flat valley floors, which becomes the fundamental factor transforming earthquake risk into a disaster. The fact that the LR model includes the surroundings of settlement areas in the moderate hazard class compared to AHP indicates that not only the fault line itself but also its immediate vicinity (near-fault effect) should be taken into account in urban transformation projects (Somerville et al., 1997).

In this study, regional scale (1:25,000 and 1:100,000) data were used. The lack of building-based structural vulnerability data (building age, material quality, etc.) is a limitation of the study. In future studies, it is recommended to conduct micro-zonation studies in high-hazard areas determined by the LR model (especially in the Erbaa-Niksar line) and to integrate the building stock inventory into the model. A limitation of this study regards the spatial resolution of the Vs30 dataset derived from the USGS global proxy. While the topographic data (FABDEM) offers high resolution (25 m), the native resolution of the Vs30 data is significantly coarser (1 km). Although resampled to match the model's pixel size, this discrepancy may result in generalized approximations of soil behavior, particularly in narrow transition zones between basin fill and bedrock. Future studies would benefit from incorporating site-specific microtremor measurements to refine these geotechnical parameters. Furthermore, to balance the subjective nature of AHP, testing the LR trained with AHP data approach applied in this study in different tectonic basins would be beneficial for introducing the method to the literature.

Etik Kurulu Onayı/***Ethics Committee Approval***: Bu çalışma için Etik Kurul onayı gerekmemektedir. *Ethics Committee Approval is not required for this study.*

Çıkar Çatışması/*Conflict of Interest*: Bu çalışmada herhangi bir çıkar çatışması bulunmamaktadır. *There is no conflict of interest in the study.*

Yazar Katkısı/*Author contributions*: Ahmet Toprak, veri toplama sürecini yönetti ve çalışmayı tasarladı. Materyal hazırlığı ve analizi Sevilay Yaşarul tarafından gerçekleştirildi. Makalenin ilk taslağı Ahmet Toprak tarafından yazıldı. Ayrıca, Ahmet Toprak nihai makaleyi gözden geçirdi ve onayladı. *Ahmet Toprak data collection, conceived and designed the study. Material preparation and analysis were carried out by Sevilay Yaşarul. The initial draft of the manuscript was authored by Ahmet Toprak. Furthermore, Ahmet Toprak reviewed and approved the final manuscript.*

Teşekkür/Acknowledgements: Yazarlar, bu çalışmada Tokat ili için kullanılan deprem verilerini sağlayan Boğaziçi Üniversitesi Kandilli Gözlemevi'ne teşekkür eder. The authors would like to thank Boğaziçi University Kandilli Observatory for providing the earthquake data used in this study for Tokat Province.

Funding: The author certifies that no financial assistance, grants, or other forms of support were obtained during the preparation of this manuscript. Yazar, bu makalenin hazırlanması sırasında herhangi bir mali yardım, hibe veya başka türde destek alınmadığını beyan eder.

References

AFAD (2024). *Deprem kataloğu*. https://deprem.afad.gov.tr/event-catalog

Akgül, A., & Akın, M. (2023). Kayseri il merkezi için Vs30 kayma dalgası hızı haritalarının hazırlanması [Yayımlanmamış yüksek lisans tezi]. Nevşehir Hacı Bektaş Veli Üniversitesi.

Akın, M., Kramer, S. L., & Topal, T. (2010). Comparison of measured and estimated shear wave velocities in a seismically active area (Erbaa, Turkey). *Proceedings of the International Conference on Recent Advances in Geotechnical Earthquake Engineering and Soil Dynamics*.

Aktaş, C., & Erkuş, O. (2009). Investigation of fog forecasting of Eskişehir using logistic regression analysis. *İstanbul Ticaret Üniversitesi Fen Bilimleri Dergisi, 8*(16), 47–61.

Alizadeh M., Mazlan H., Esmaeil A., Himan S., Mohammad R. K., Amin B. P., Biswajeet P., Hassan Z. (2018). Multi-criteria decision making (MCDM) model for seismic vulnerability assessment (SVA) of urban residential buildings. *ISPRS International Journal of Geo-Information 7* (11). https://doi.org/10.3390/ijgi7110444.

Alkan, H., Toker, M., & Akkaya, İ. (2023). Van Gölü havzası ve civarının depremselliğine genel bir bakış. *Yüzüncü Yıl Üniversitesi Fen Bilimleri Enstitüsü Dergisi*, *28*(1), 317-333. https://doi.org/10.53433/yyufbed.1138320

Alpaslan, N. (2013). Zemin sıvılaşması ve mekanizması. *Batman Üniversitesi Yaşam Bilimleri Dergisi*, *3*(2), 67-89.

Ambraseys, N.N. (1970). Some characteristic features of the Anatolian fault zone. *Tectonophysics, 9*, 143-165.

Ansal, A., Kurtuluş, A., & Tönük, G. (2010). Seismic microzonation and earthquake damage scenarios for urban areas. *Soil Dynamics and Earthquake Engineering*, *30*(11), 1319-1328. https://doi.org/10.1016/j.soildyn.2010.06.004

Ardos, M. (1995) *Türkiye Ovalarının Jeomorfolojisi*. Cilt:1 2. Baskı Çantay Kitabevi.

Arnold, C. (2006). *Risk Management Series: Designing for Earthquakes*. FEMA. Oakland, Kaliforniya.

Bahadori, H., Hasheminezhad, A., & Karimi, A. (2017). Development of an integrated model for seismic vulnerability assessment of residential buildings: Application to Mahabad City, Iran. *Journal of Building Engineering, 12*, 118-131. https://doi.org/10.1016/j.jobe.2017.05.014

Barka, A. (1996) Slip distribution along the North Anatolian fault associated with the large earthquakes of the period 1939 to 1967. *Bulletin of the Seismological Society of America*, *86*(5), 1238-1254. https://doi.org/10.1785/BSSA0860051238

Barka, A.A. (1992), The north Anatolian fault zone. In *Annales tectonicae. 6*, 164-195.

Barka, A., Akyüz, H. S., Cohen, H. A., & Watchorn, F. (2000). Tectonic evolution of the Niksar and Tasova–Erbaa pull-apart basins, North Anatolian Fault Zone: their significance for the motion of the Anatolian block. *Tectonophysics*, *322*(3-4), 243-264. https://doi.org/10.1016/S0040-1951(00)00099-8

Bulut, A. (2023). Bireylerin afet okuryazarlığı düzeylerini etkileyen faktörlerin sıralı lojistik regresyon analizi ile incelenmesi. *Afet ve Risk Dergisi*, *6*(3), 691-709. https://doi.org/10.35341/afet.1297045

Cankar, S. (2014). *Kazova'da arazi bozulmasına hassas alanların belirlenmesi ve haritalanması* [Yayımlanmamış yüksek lisans tezi]. Gaziosmanpaşa Üniversitesi.

Canpolat, F. A., & Bulucu, Y. (2024). Kayseri ilindeki deprem tehlikesinin sezgisel ve istatistiksel modeller kullanılarak karşılaştırmalı analizi. *Türk Coğrafya Dergisi, 86*, 143–159. https://doi.org/10.17211/tcd.1556195

Çatkın, Ş & Toprak, A. (2025). Integrated seismic risk assessment using multi-criteria decision making, statistical, and machine learning approaches: a case study of Denizli, Türkiye. *Natural Hazards*, 1-31. https://doi.org/10.1007/s11069-025-07674-6

Demir, M., & Altaş, N. T. (2024). Kars kentinde deprem hasar risk potansiyeli taşıyan alanların CBS tabanlı AHP analizlerine dayalı olarak belirlenmesi. *Geomatik*, *9*(1), 123-140. https://doi.org/10.29128/geomatik.1375650

Emre, Ö., Duman, T. Y., Özalp, S., Elmacı, H., Olgun, Ş., & Şaroğlu, F. (2013). *Açıklamalı Türkiye Diri Fay Haritası.* Ölçek 1:1.250.000. Ankara, Türkiye: Maden Tetkik ve Arama Genel Müdürlüğü, Özel Yayın Serisi-30. Türkiye. ISBN: 978-605-5310-56-1

Erinç, S. (2000). *Jeomorfoloji-I*. *Der* Yayınları.

Eyidoğan, H., Güçlü, U., Utku, Z., & Değirmenci, E. (1991). *Türkiye büyük depremleri makro-sismik rehberi* (1900-1988). *İTÜ MF* Jeofizik Mühendisliği Bölümü Yayınları, 200.

Harff, J., Meschede, M., Petersen, S., & Thiede, J. (Eds.). (2016). *Encyclopedia of marine geosciences*. Springer. https://doi.org/10.1007/978-94-007-6238-1

Hawker, L., Uhe, P., Paulo, L., Sosa, J., Savage, J., Sampson, C., & Neal, J. (2022). A 30 m global map of elevation with forests and buildings removed. *Environmental Research Letters*, *17*(2), 024016. https://dx.doi.org/10.1088/1748-9326/ac4d4f

He W, Chen G, Zhao J, Lin Y, Qin B, Yao W, Cao Q (2023). Landslide susceptibility evaluation of machine learning based on information volume and frequency ratio: a case study of Weixin County, China. *Sensors* *23*(5):2549. https://doi.org/10.3390/s23052549

Hu, J., Chen, J., Chen, Z., Cao, J., Wang, Q., Zhao, L., Zhang, H., Xu, B. & Chen, G. (2018). Risk assessment of seismic hazards in hydraulic fracturing areas based on fuzzy comprehensive evaluation and AHP method (FAHP): A case analysis of Shangluo area in Yibin City, Sichuan Province, China. *Journal of Petroleum Science and Engineering*, *170*, 797-812. https://doi.org/10.1016/j.petrol.2018.06.066

Hubert-Ferrari, A., Armijo, R., King, G., Meyer, B., & Barka, A. (2002). Morphology, displacement, and slip rates along the North Anatolian Fault, Turkey. *Journal of Geophysical Research: Solid Earth*, *107*(B10), ETG-9.

Işık, E., Karasin, İ. B., & Ulu, A. E. (2020). Eğimli Zeminlerde İnşa Edilen Betonarme Binaların Deprem Davranışlarının İncelenmesi. *Avrupa Bilim ve Teknoloji Dergisi*, (20), 162-170. https://doi.org/10.31590/ejosat.757763

JRC. (2018). *GHS-BUILT-H R2022A-GHS building height, derived from AW3D30, SRTM30, and Sentinel2 composite* (2018)-OBSOLETE RELEASE. https://data.jrc.ec.europa.eu/dataset/ce7c0310-9d5 e-4aeb-b99e-4755f6062557

Kalman Šipoš, T., Brandis, A., Bohinc, U., & Ristić, U. (2025). Determining Critical Ground Motion Parameters for Damage Prediction in Reinforced Concrete Frame Existing Buildings. *Applied Sciences* (2076-3417), *15*(5).

Kanık, E. A., & Erden, S. (2003). Tanı testlerinin değerlendirilmesinde ROC (Receive Operating Characteristics) eğrisinin kullanımı. *Mersin Üniversitesi Tıp Fakültesi Dergisi*, *3*, 260-264.

Kiper, P. (2001). Doğal Afet Planlama İlişkisi. *Planlama Dergisi, 3*, 4-16.

Li, S., & Shen, L. (2024). Seismic optimization design and application of civil engineering structures integrated with building robot system technology. *HighTech Innovation Journal, 5*(4), 1118–1134. https://doi.org/10.28991/HIJ-2024-05-04-017

Liberatore, M. J. & Nydick, R. L. (1990), "An Analytic Hierarchy Approach for Evaluating Product Formulations", Chapter 7, *Computer Aided Formulation: A Manual for Implementation, VCH Publishing Company*, New York,

Marangoz, M., & İzci, Ç. (2023). Doğal afetlerin ekonomik, sosyal ve çevresel etkilerinin 6 Şubat 2023 Kahramanmaraş merkezli depremler bağlamında girişimciler açısından değerlendirilmesi. *Sosyal ve Beşeri Bilimler Araştırmaları Dergisi*, *24*(52), 1-30.

Meunier, P., Hovius, N., & Haines, AJ. (2007). Regional patterns of earthquake-triggered landslides and their relation to ground motion. *Geophysical Research Letters*, *34*(20). https://doi.org/10.1029/2007GL031337

Mhaske, S. Y., & Choudhury, D. (2010). GIS-based soil liquefaction susceptibility map of Mumbai city for earthquake events. *Journal of Applied Geophysics*, *70*(3), 216-225. https://doi.org/10.1016/j.jappgeo.2010.01.001

Nazmfar, H. (2019). An integrated approach of the analytic network process and fuzzy model mapping of evaluation of urban vulnerability against earthquake. Geomatics, *Natural Hazards and Risk.*

https://doi.org/10.1080/19475705.2019.1588791

Ocak, F. & Bahadır, M. (2022). CBS teknikleri kullanılarak deprem duyarlılık analizi için Analitik Hiyerarşi Prosesi: Samsun Ladik Gölü Havzası örneği, Türkiye. *Kesit Akademi Dergisi*, *8* (33), 322-348.

Ochoa, L. H., Niño, L. F., Vargas, C. A. (2018). Fast estimation of earthquake epicenter distance using a single seismological station with machine learning techniques. *Dyna*, *85*(204), 161-168.

Orhan, M., & Ateş, A. (2011). Koni Penetrasyon Testi (CPT) Verileri ile Zeminlerin Sıvılaşma Potansiyelinin Manisa-Saruhanlı Örneği ile Araştırılması. *Politeknik Dergisi*, *14*(1), 15-23.

Özbek, A. (2017). Çok kriterli karar verme yöntemleri ve excel ile problem çözümü. *Seçkin Yayıncılık,* Ankara, 197.

Özkazanç, S. (2015, 14-16 Ekim). *Sosyal, mekânsal ve ekonomik boyutlarıyla afetzede konutları* [Sözlü bildiri]. 3. Türkiye Deprem Mühendisliği ve Sismoloji Konferansı.

Özmen, B., Güler, H., & Nurlu, M. (1997). *Coğrafi bilgi sistemi ile deprem bölgelerinin incelenmesi.* Bayındırlık ve İskan Bakanlığı Afet İşleri Fenel Mürdürlüğü.

Özşahin, E. (2014). Earthquake damage risk analysis in Tekirdağ province using Geographic Information Systems (GIS) and Analytic Hierarchy Process (AHP). *International Journal of Human Sciences*, *11*(1), s. 861-879. http://dx.doi.org/10.14687/ijhs.v11i1.2816

Özüpekçe S, & Deniz, Ö. (2023). Türkiye'nin depremselliği ve sosyo-ekonomik etkileri 6 şubat depremleri örneği. M. Bulut ve Z. Karacagil (Ed.) *Sosyal Bilimlerde Güncel Tartışmalar* (s. 544-573).

Pal, I., Nath, S. K., Shukla, K., Pal, D. K., Raj, A., Thingbaijam, K. K. S., & Bansal, B. K. (2008). Earthquake hazard zonation of Sikkim Himalaya using a GIS platform. *Natural Hazards, 45*, 333–377.https://doi.org/10.1007/s11069-007-9173-7

Panahi, M., Rezaie, F., & Meshkani, S. A. (2014). Seismic vulnerability assessment of school buildings in Tehran city based on AHP and GIS. *Natural Hazards and Earth System Sciences*, *14*(4), 969-979. https://doi.org/10.5194/nhess-14-969-2014

Pourghasemi, H. R., Pradhan, B., & Gokceoglu, C. (2012). Application of fuzzy logic and analytical hierarchy process (AHP) to landslide susceptibility mapping at Haraz watershed, Iran. *Natural hazards*, *63*(2), 965-996. https://doi.org/10.1007/s11069-012-0217-2

Pranowo, Makrup L, Pawirodikromo W, Muntafi, Y. (2024). Comparison of structural response utilizing probabilistic seismic hazard analysis and design spectral ground motion. *Civil Eng J* *10*:235–251. https://doi.org/10.28991/CEJ-SP2024-010-012

Rehman, A., Sajjad, M., Song, J., Riaz, M.T., Mehmood, M.S., Ahamad, M.I. (2024). Integrated frequency ratio-analytical hierarchy and geospatial techniques-based earthquake risk assessment in mountainous cities: a case from the Northwestern Himalayas. *Georisk: Assessment and Management of Risk for Engineered Systems and Geohazards.* https://doi.org/10.1080/17499518.2024.2378285

Ren, T., Wang, Z., Ma, Y., Yan, J., Liu, K., & Li, H. (2024). Study of an evaluation method of earthquake-proof capacity of a community during an earthquake. *Frontiers in Earth Science*, *12*, 1366697. https://doi.org/10.3389/feart.2024.1366697

Robertson, P. K., & Wride, C. E. (1998). Evaluating cyclic liquefaction potential using the cone penetration test. *Canadian geotechnical journal*, *35*(3), 442-459. https://doi.org/10.1139/t98-017

Rusydi, M., & Efendi, R. (2018). Earthquake hazard analysis use Vs30 data in Palu. *In Journal of Physics: Conference Series* (Vol. *979*, No. 1, p. 012054). IOP Publishing.

Saaty, T. L. (1980). The analytic hierarchy process (AHP). *The Journal of the Operational Research Society, 41*(11), 1073-1076.

Shafapourtehrany, M., Yariyan, P., Özener, H., Pradhan, B., & Shabani, F. (2022). Evaluating the application of K-mean clustering in earthquake vulnerability mapping of Istanbul, Turkey. *International Journal of Disaster Risk Reduction,* *79*, 103154. https://doi.org/10.1016/j.ijdrr.2022.103154

Siyahi, B., Çetin, K. Ö., & Bilge, H. T. (2013). Geoteknik deprem mühendisliği açısından zemin-temel-yapı etkileşimine kritik bakış. *Türkiye Mühendislik Haberleri*, *484*, 41-50

Somerville, P. G., Smith, N. F., Graves, R. W., & Abrahamson, N. A. (1997). Modification of empirical strong ground motion attenuation relations to include the amplitude and duration effects of rupture directivity. *Seismological research letters*, *68*(1), 199-222. https://doi.org/10.1785/gssrl.68.1.199

Sönmez, M. E. (2011). Coğrafi Bilgi Sistemleri (CBS) Tabanlı Deprem Hasar Riski Analizi: Zeytinburnu (İstanbul) Örneği, *Türk Coğrafya Dergisi, 56*, 11-22.

Susam, T., Esmeray, A., Öztoprak, B., Yaprak, S., & Toprak, Ö. (2011). CBS ile Yeşilırmak Nehir Yatağı Tokat merkez bölümünde deprem riskinin irdelenmesi. *İTÜ Dergisi/d*, *5*(3).

Sunbul, F., Karadeniz, E., Sengun, M. T., & Kocaoglu, M. (2025). Forecasting urban shifts post-earthquake: LULC change analysis in Elazığ, Turkey using ANN and Markov models. The *Geographical Journal*, e70022. https://doi.org/10.1111/geoj.70022

Şaroğlu, F., Emre, O., & Kuscu, I. (1992). *Active fault map of Turkey*. General Directorate of Mineral Research and Exploration.

Şeker, B.D. (2023). Doğal afetlerin göç üzerindeki etkiler: Depremler ve Türkiye. *Göç Dergisi*, *10*(2), 173–187.

Şengör, A.M.C., (1979). The North Anatolian transform fault: its age, offset and tectonic significance. *Journal of Geological Society of London, 136*, 269-282.

Şengör, A. M. C., Görür, N. and Şaroğlu, F., (1985). Strike-slip faulting and related basin formation in zones of tectonic escape: Turkey as a case study, Strike-slip deformation, basin formation, and sedimentation, *Soc. Econ. Paleont*. Min. Spec. Pub. *37* (in honor of J.C. Crowell), 227-264.

Şengör, A. M. C., Tüysüz, O., Imren, C., Sakınç, M., Eyidoğan, H., Görür, N., Le Pichon, X & Rangin, C. (2005). The North Anatolian fault: A new look. *Annual Review of Earth and Planetary Sciences*, *33*(1), 37-112.

Şengün, M. T., Idrısheva, Z., Siler, M., & Karadeniz, E. (2018). *Palu'da (Elazığ) depremsellik ve yerleşim alanı risk değerlendirmesi*. Uluslararası Palu Sempozyumu.

Tatar, O., Gürsoy, H., Koçbulut, F., Kavak, K. Sezen, T. F., Polat, A., Akpınar, Z., & Mesci, L. O. (2006). *Kuzey Anadolu Fay Zonu-1942 Erbaa-Niksar depremi yüzey kırığı: Yeni gözlemler.* Atag10-Aktif Tektonik Araştırma Grubu, 10.

Toprak, A., & Günek, H. (2016). Flood analysis of arakonak stream basin (Solhan-Bingöl). *Recent Research in Interdisciplinary Sciences*, *358*.

Toprak A, Sunkar M. (2022). Ağrı İlinde Meydana Gelen Doğal afetlerin Mekânsal ve Zamansal analizi. *Coğrafya Dergisi*. *44*, 97-113. https://doi.org/10.26650/JGEOG2022-978387

Tudes, S. (2012). Correlation between geology, earthquake and urban planning. *Earthquake Research and Analysis-Statistical Studies, Observations and Planning*, p. 417-434

Triollet, R., Mccafferty, E., Alvarez Martinez, A., Bellan, E., Kennedy, P. and Al Khudhairy, D., (2018) *JRC Annual Report 2018*, Publications Office of the European Union, Luxembourg, 2019, ISBN 978-92-76-00655-8. https://doi.org/10.2760/197350

UNISDR (2015). *Sendai Framework for Disaster Risk Reduction 2015–2030.* United Nations International Strategy for Disaster Reduction.

USGS, (2023), *U.S. Geological Survey. (2023). Earthquake lists, maps, and statistics.* https://www.usgs.gov/natural-hazards/earthquake-hazards/lists-maps-and-statistics

Üzen, İ. (2014). 1942 ve 1943 Erbaa Depremleri. *Karadeniz Araştırmaları*, (40), 77-93.

Varnes, D. J. (1984). *Landslide Hazard Zonation: A Review of Principles and Practice*. UNESCO, Paris.

Wang, Q., & Li, W. (2017). A GIS-based comparative evaluation of analytical hierarchy process and frequency ratio models for landslide susceptibility mapping. *Physical Geography, 38*(4), 318-337.

Xie, P., Wen, H., Ma, C., Baise, L. G., & Zhang, J. (2018). Application and comparison of logistic regression model and neural network model in earthquake-induced landslides susceptibility mapping at mountainous region, China. *Open Geosciences, 10*(1), 162–175. https://doi.org/10.1080/19475705.2018.1451399

Yavaşoğlu, F., & Özden, Ç. V. (2017). Coğrafi Bilgi Sistemleri Tabanlı Analitik Hiyerarşi Süreci Kullanılarak Deprem Hasar Riski Analizi: Kadıköy Örneği. *Tübav Bilim Dergisi*, *10*(3), 28-38.

Yoloğlu, A. C., & Zorlu, F. (2024). Türkiye'de deprem riski ile ilişkili olarak bölgesel yığılma ve eşitsizlikler. *Sketch: Journal of City and Regional Planning*, *6*(01), 78-96.

Yunus, A. P., Xinyu, C., Catani, F., Subramaniam, S. S., Fan, X., Jie, D., K. S. Sajinkumar, Ankita Gupta & Avtar, R. (2023). Earthquake-induced soil landslides: volume estimates and uncertainties with the existing scaling exponents. *Scientific Reports*, *13*(1), 8151. https://doi.org/10.1038/s41598-023-35088-6